JMEPEG (1998) 7:682-690

The Effects of Artificial Aging on the Microstructure and Fracture Toughness of Al-Cu-Li Alloy 2195

P.S. Chen, A.K. Kuruvilla, T.W. Malone, and W.P. Stanton

(Submitted 19 February 1998; in revised form 11 May 1998)

Aluminum-lithium alloys have shown promise for aerospace applications, and National Aeronautics and Space Administration (NASA) has selected the aluminum-lithium Alloy 2195 for the main structural alloy of the super light weight tank (SLWT) for the space shuttle. This alloy has significantly higher strength than conventional 2*xxx* alloys (such as 2219) at both ambient and cryogenic temperatures. If properly processed and heat treated, this alloy can display higher fracture toughness at cryogenic temperature than at ambient temperature. However, the properties of production materials have shown greater variation than those of other established alloys, as is the case with any new alloy that is being transitioned to a demanding application.

Recently, some commercial 2195 plates for the SLWT program were rejected, mostly due to low CFT or FTR at ambient and cryogenic temperatures. Investigation of the microstructure property relationships of Al-Cu-Li based alloys indicates that the poor fracture toughness properties can be attributed to excessive T_1 precipitation at subgrain boundaries. Lowering the aging temperature is one way to avoid excessive T_1 precipitation at subgrain boundaries. However, this approach results in a significant drop in yield strength. In addition, low-temperature aging is associated with sluggish aging kinetics, which are not desirable for industrial mass production. Therefore, the present study was undertaken to develop an aging process that can improve fracture toughness without sacrificing yield and tensile strength.

A multistep heating-rate controlled (MSRC) aging treatment has been developed that can improve the cryogenic fracture toughness of aluminum-lithium Alloy 2195. At the same levels of yield strength (YS), this treatment results in considerably higher fracture toughness than that found in Alloy 2195, which has received conventional (isothermal) aging. Transmission electron microscopy revealed that the new treatment greatly reduces the size and density of subgrain-boundary T_1 precipitates. In addition, it promotes T_1 and θ'' nucleation, resulting in a fine and dense distribution of precipitate particles in the matrix. The MSRC aging treatment consists of (a) aging at 127 °C (260 °F) for 5 h, (b) heating continuously from 127 °C (260 °F) to 135 °C (275 °F) at a rate of 0.556 °C/h (1 °F/h), (c) holding at 135 °C (275 °F) for 5 h, (d) heating continuously from 135 to 143 °C (275 to 290 °F) at a rate of 0.556 °C/h (1 °F/h), and (e) holding at 143 °C (290 °F) for 25 h to obtain a near peak-aged condition.

Keywords Alloy 2195, aluminum, heat treatment, lithium alloys, microstructure, spacecraft hardware

1. Introduction

The National Aeronautics and Space Administration (NASA) has selected aluminum-lithium Alloy 2195 to be the main structural alloy of the super light weight tank (SLWT) for the space shuttle. This alloy has significantly higher strength than conventional 2*xxx* alloys (such as 2219) at both ambient and cryogenic temperatures. If properly processed and heat treated, this alloy can display higher fracture toughness at cryogenic temperature than at ambient temperature. However, the properties of production materials have shown greater variation than those of other established alloys, as is the case with any new alloy that is being transitioned to a demanding application. Cryogenic strength and toughness are critical to this application, because the SLWT will house liquid oxygen and hydrogen. To ensure proper quality control, NASA has imposed a lot acceptance testing on Alloy 2195 plate before it can be used in the SLWT program. During lot acceptance testing, strength and toughness are measured at ambient and cryogenic temperatures in relevant positions and orientations. One guideline for lot acceptance is that Alloy 2195 must have a fracture toughness ratio (FTR) greater than one. (Here, FTR is the ratio of fracture toughness at cryogenic temperature compared to that at ambient temperature.) It is equally important that the alloy has higher strength and toughness at cryogenic temperatures than at ambient temperature in order to avoid expensive cryogenic proof testing.

Previous studies have shown that good compositional control (Ref 1, 2), thermomechanical processing (TMP), and aging treatments can produce an FTR > 1 in Alloy 2195 (Ref 2). However, Alloy 2195 has exhibited lot-to-lot variations in strength and toughness after conventional isothermal aging, which can be attributed to the combined effects of variations in chemical composition and thermomechanical processing. One recent study (Ref 2) indicated that cryogenic fracture toughness (CFT) is related to the density, size, and location of a par-

P.S. Chen and **A.K. Kuruvilla,** IIT Research Institute, Metallurgy Research Facilities, Building 4628, Marshall Space Flight Center, AL 35812; **T.W. Malone** and **W.P. Stanton,** National Aeronautics and Space Administration, Materials and Processes Laboratory, Metals Processing Branch, Marshall Space Flight Center, AL 35812.

ticular precipitate found in these alloys and labeled as T_1. Cryogenic fracture toughness decreases considerably as T_1 precipitates increase in density at the subgrain boundaries and in size in the matrix (Ref 2). This trend (in the variation of toughness with the distribution of T_1 precipitates at subgrain boundaries) has also been observed in other aluminum-lithium alloys (Ref 3, 4). Therefore, attempts to improve fracture toughness were directed toward reducing the density of T_1 precipitates at subgrain boundaries and enhancing the nucleation of T_1 precipitates in the matrix.

This study details a new aging treatment that improves cryogenic fracture toughness by controlling the location and size of the major strengthening precipitate, T_1. The new treatment uses multistep heating-rate controlled (MSRC) aging to prevent T_1 from precipitating preferentially at the subgrain boundaries. In addition, the new aging treatment can minimize variations in mechanical properties due to variations in TMP parameters and alloy chemistry. This paper discusses MSRC aging treatment, correlating microstructure to observed improvements in cryogenic fracture toughness.

2. Technical Approach

This study used an alloy that had yield strength (YS) >503 MPa (73 ksi) and that displayed an FTR <1 after isothermal aging (Ref 2) (Fig. 1). In Al-Cu-Li alloys, FTR correlates well with the degree of T_1 precipitation at subgrain boundaries (Fig. 2). Fracture toughness ratio may also correlate with the size and density of T_1 precipitates in the matrix (Ref 2) (Fig. 3). High cryogenic fracture toughness can be achieved by suppressing T_1 precipitation at subgrain boundaries and enhancing T_1 nucleation in the matrix, thus eliminating premature fracture along precipitate-rich subgrain boundaries.

In Al-Cu-Li alloys, T_1 particles generally precipitate heterogeneously on matrix dislocations and/or subgrain boundaries, depending on aging temperatures and duration (Ref 3). In Alloy X2095, which is similar to Alloy 2195, lower aging temperature was found to prevent T_1 precipitation at subgrain boundaries (Ref 3), which was explained on the basis of the equation for the heterogeneous nucleation rate (N_{het}) (Ref 5):

$$N_{het} = \omega C_1 \exp\left(\frac{-\Delta G_m}{kT}\right) \cdot \left(\frac{-\Delta G^*}{kT}\right) \text{nuclei m}^{-3}\text{s}^{-1} \qquad \text{(Eq 1)}$$

where N_{het} is heterogeneous nucleation rate, α is a factor that includes vibration frequency of atoms and area of critical nucleus, C_1 is concentration of nucleation sites per unit volume, ΔG_m is activation energy for diffusion, ΔG^* is activation energy barrier required to form critical-sized nuclei, k is Boltzmann constant, and T is temperature (K).

When the alloy composition is fixed, Eq 1 indicates that the heterogeneous nucleation rate is greatly dependent on C_1 and ΔG^*.When arranged in decreasing order, the sequence of ΔG^* would be roughly (1) homogeneous sites, (2) vacancies, (3) dislocations, (4) stacking faults, (5) grain boundaries and interphase boundaries, and (6) free surfaces.

It is believed that T_1 nucleation on matrix dislocations requires more activation energy than nucleation on subgrain boundaries in Alloy 2195. However, matrix nucleation sites generally outnumber subgrain boundary sites, especially when the alloy is stretched prior to aging. With low undercooling (high-activation barrier, high-aging temperature), nucleation rates will be highest at sites requiring little activation energy,

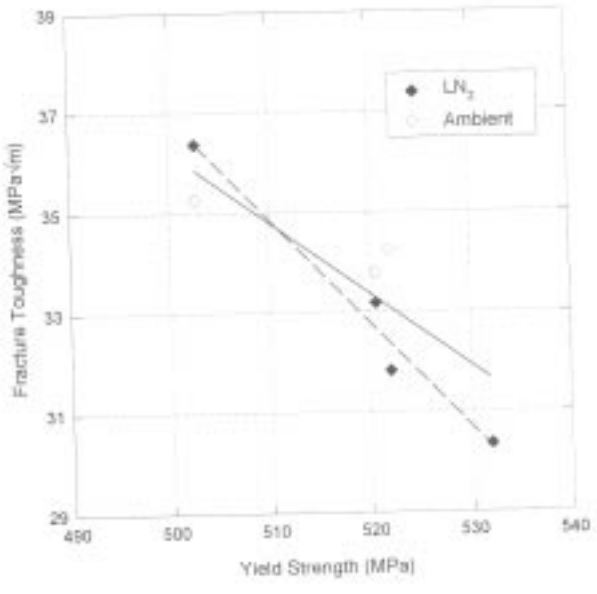

Fig. 1 Fracture toughness versus yield strength in conventionally aged Alloy 2195 at ambient and cryogenic temperatures (Ref 2)

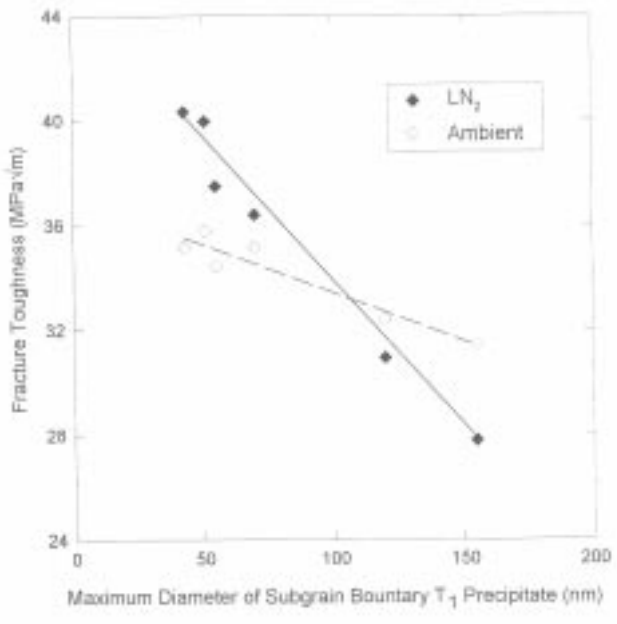

Fig. 2 Fracture toughness versus maximum size of T_1 at subgrain boundaries, with fracture toughness decreasing as T_1 size increases (Ref 2)

such as grain and subgrain boundaries. As the undercooling increases (low-activation barrier, low-aging temperature), higher nucleation rates will be seen at sites that have the highest concentration of nucleation sites. Therefore, by lowering the aging temperature, matrix dislocations become favorable nucleation sites, and T_1 nucleation at subgrain boundaries can be restrained.

However, low-temperature aging is associated with sluggish aging kinetics, which are not desirable for industrial production. Furthermore, it is not clear whether a low-aging temperature can sufficiently strengthen the alloy while improving its fracture toughness. Therefore, an urgent need existed to develop a new aging treatment that could improve cryogenic fracture toughness while retaining yield strength (YS) at a level of 517 to 538 MPa (75 to 78 ksi) and aging the properties within a reasonable length of time.

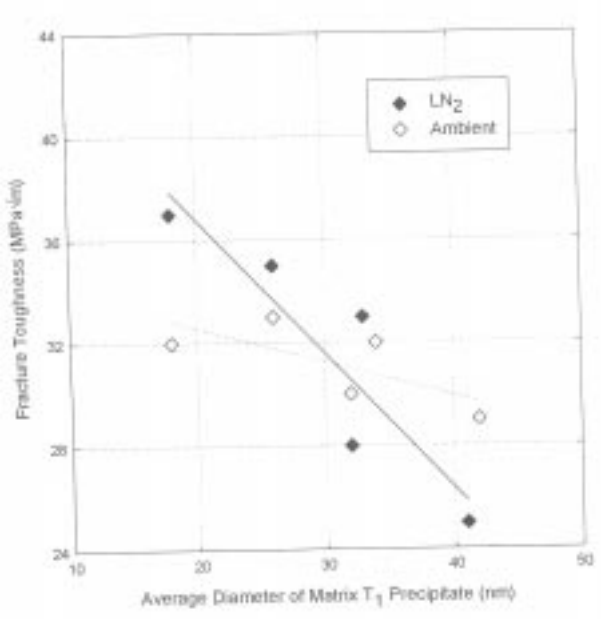

Fig. 3 Correlation of cryogenic fracture toughness with size of matrix T_1 precipitates (Ref 2)

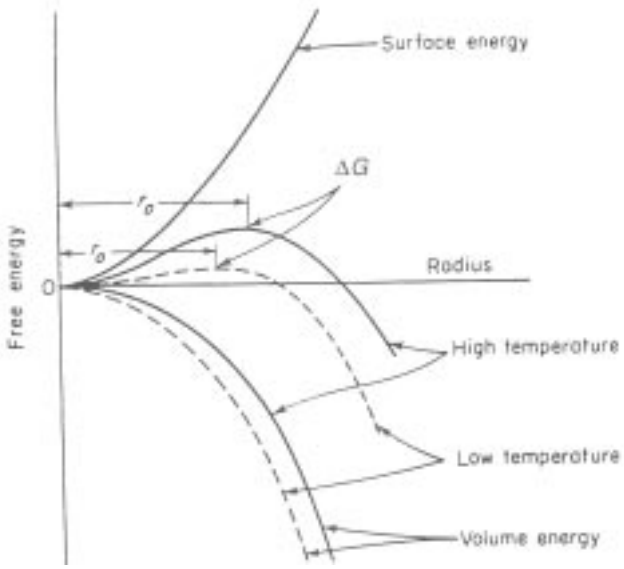

Fig. 4 Effects of precipitation temperature on free energy of a precipitate particle as a function of its radius (Ref 6)

Precipitation of strengthening phases requires a free-energy change of the system, as expressed by the following equation (Ref 6):

$$\Delta G = -\Delta G_v + \Delta G_s + \Delta G_m \quad \text{(Eq 2)}$$

where ΔG_v is volume free energy, ΔG_s is surface free energy, and ΔG_m is free energy of strain due to formation of precipitate particle. The surface free energy varies with the area of the particle, while volume free energy varies with the volume of the particle. Assuming a spherical particle and $\Delta G_m = 0$, Eq 2 can therefore be written as:

$$\Delta G = -A_1 r^3 + A_2 r^3 \quad \text{(Eq 3)}$$

where A_1 and A_2 are constants and r is radius of the embryo.

Figure 4 shows a plot of Eq 3. The total free energy is positive when the particle radius is small, because the surface free energy is larger than the volume free energy. However, the total free energy becomes negative as the radius increases.

A particle with a radius less than the critical radius (r_0) tends to dissolve in the solid solution, while a particle with a radius larger than r_0 tends to grow continuously because the free energy is reduced as it grows. The size of a stable nucleus (critical radius) varies with temperature. As the temperature is lowered, the critical radius for precipitate nucleation rapidly decreases in size, as does the energy necessary to form this critical embryo.

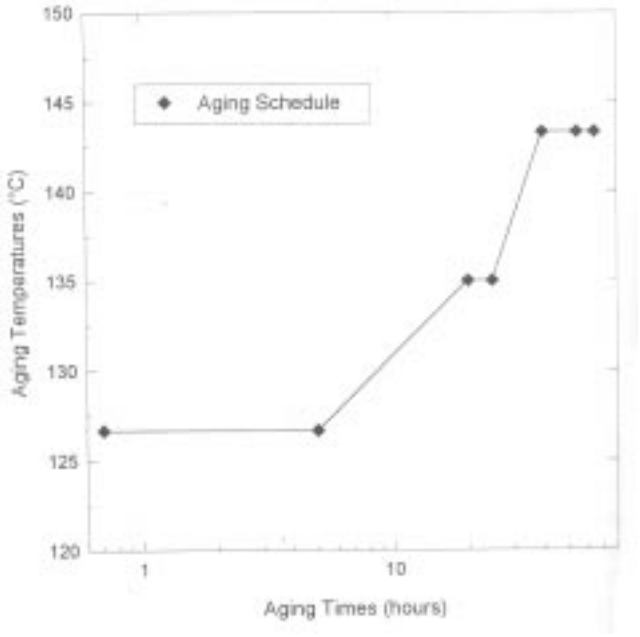

Fig. 5 Schedule for multistep heating-rate controlled aging treatment

Therefore, decreasing temperature correlates with an increase in the total number of embryos that can precipitate.

Based on this theory, a MSRC aging treatment was developed to promote T_1 nucleation and growth in the matrix, rather than at subgrain boundaries (Fig. 5). Aging begins with initial holding at low temperature (with high undercooling) to enhance formation of T_1 nuclei in the matrix. Then the furnace temperature is gradually increased 0.556 °C/h (1 °F/h) to permit each precipitate nuclei to grow above r_0 and become a stable nucleus. These nuclei continue to grow during aging, with negligible dissolution into solid solution. Long-term aging at low temperatures also allows T_1 precipitates to grow in the matrix before they can nucleate and grow at the subgrain boundaries.

As temperatures continue to rise, T_1 eventually nucleates at subgrain boundaries and begins to grow. However, this treatment reduces time at the highest aging temperature. Thus, T_1 precipitates are permitted to nucleate and grow in the matrix before precipitation occurs at the subgrain boundaries. Early growth of T_1 precipitates in the matrix greatly reduces copper and lithium concentrations adjacent to the subgrain boundaries, hindering the growth of subgrain boundary T_1. At the subgrain boundaries, T_1 precipitates will be smaller and more scarce than those seen in Alloy 2195, which has experienced isothermal aging.

In short, this MSRC aging treatment is significant in that T_1 is allowed to nucleate preferentially in the matrix (where it grows steadily without dissolution), while T_1 precipitation at the subgrain boundaries is delayed and its coarsening kinetics decreased.

3. Experimental Procedures

Four lots of Alloy 2195 (Al-4.19Cu-0.95Li-0.29Mg-0.31Ag-0.12Zr) were received in the form of 1.7 in. thick rolled plates, which were then solutionized and stretched for 3% at ambient temperature. Specimens were aged at various temperatures and times to obtain acceptable toughness combined with a minimum YS of 503 MPa (73 ksi) (Table 1). Tensile tests were performed at ambient temperature, using flat tensile specimens to permit evaluation of the effect of microstructural variation through the plate thickness. The uniaxial tensile properties of the plates were evaluated in the L-T orientation (specimen axis perpendicular to the rolling direction). At least two tests were performed in each condition.

Table 1 Aging treatment for Alloy 2195 (lot A)

Treatment No.	Stretch, %	Aging treatment
1	3	SHT + 148 °C/18 h
2	3	SHT + 143 °C/30 h
3	3	SHT + 143 °C/26 h
4	3	SHT + 127 °C/5 h + TR to 135 °C (0.56 °C/h) + 135 °C/5 h + TR to 143 °C (0.56 °C/h) + 143 °C/25 h
5	3	SHT + 127 °C/5 h + TR to 135 °C (0.56 °C/h) + 135 °C/5 h + TR to 143 °C (0.56 °C/h) + 143 °C/15 h

SHT, solution heat treat; TR, temperature ramp

Fracture toughness tests were performed at ambient temperature and –196 °C (–320 °F). The plates were evaluated in the T-L orientation (notch parallel to the rolling direction), per ASTM E 740. The specimens were fatigue precracked at 20 Hz, then tensile tested to failure at a crosshead speed of 0.13 cm/min. Precrack length and maximum load to failure were factored into the standard equation.

Microstructural characterization was carried out using a JEOL 2000F (JEOL USA, Inc., Peabody, MA) transmission electron microscope (TEM) operated at 200 kV. Samples were jet polished in an electrolyte (70% methanol-30% nitric acid) at –20 °C (–4 °F), with an applied potential of 12 V. Precipitates were examined using selected area diffraction, as well as bright and dark field techniques. Matrix and subgrain boundary precipitates were examined using a beam direction near (110). Two T_1 variants

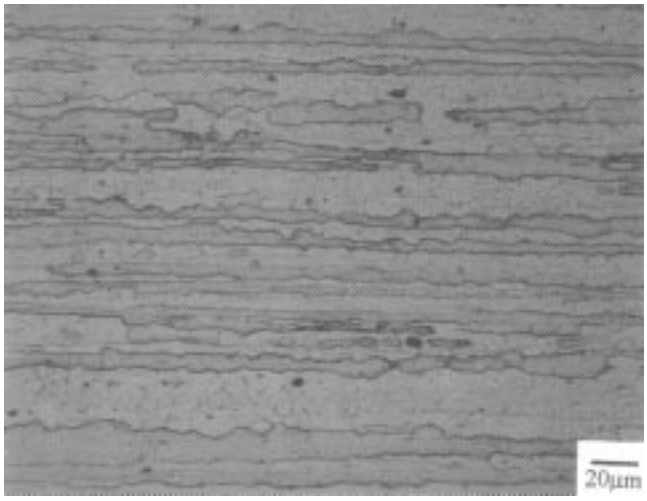

Fig. 6 Micrograph of Alloy 2195 plate, showing pancake-shaped structures in grain microstructure. 500×. (Art has been reduced to 75% of its original size for printing.)

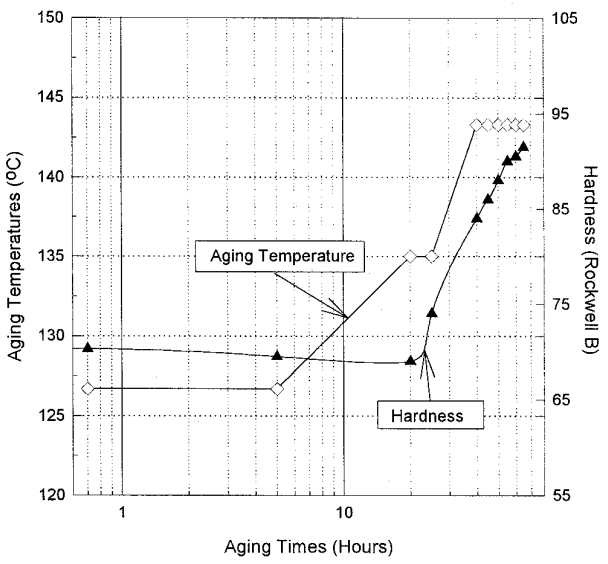

Fig. 7 Hardness increases as aging time increases for Alloy 2195 with multistep heating-rate controlled aging

and one θ′ (or θ′′) variant were oriented edge on to the beam, so that their size and distribution could be readily determined.

4. Results

4.1 Aging Response and Microstructure

The Alloy 2195 plate had a grain structure that was unrecrystallized, coarse, and pancake shaped, with dimensions ~50 μm thick, ~500 μm wide, and several millimeters long in the rolling direction (Fig. 6). Figure 7 gives hardness variation as a function of aging treatment, which shows that the hardness values peaked at different times and that the shape of the hardness curves were quite different. Transmission electron microscopy examination indicated that MSRC aging changed the size and distribution of strengthening precipitates in the matrix.

Transmission electron microscopy was also used to investigate microstructures produced by conventional and MSRC aging. The matrix contained T_1 (Al_2CuLi), θ′ (Al_2Cu), θ′′ (Al_2Cu), β′ (Al_3Zr), δ′ (AlLi), and S′ (Al_2CuMg), with T_1 as the primary strengthening phase. All matrix microstructures were similar. However, selected area diffraction patterns showed that MSRC aging produced much stronger diffracted streaking intensities of θ′′ than conventional aging (Fig. 8). Transmission

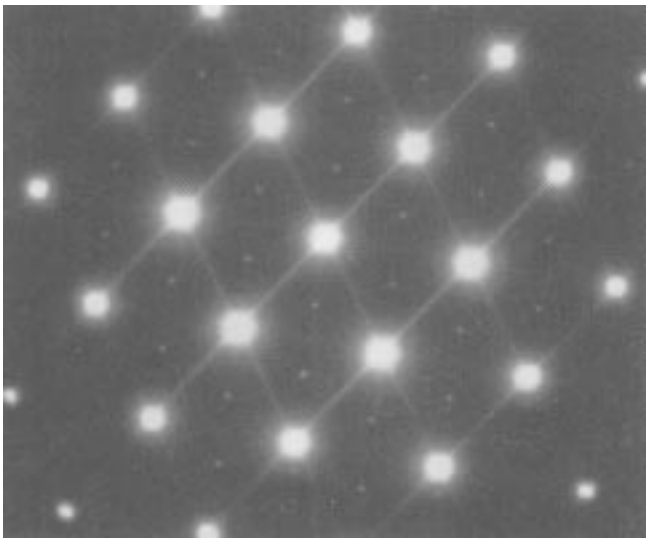

(a)

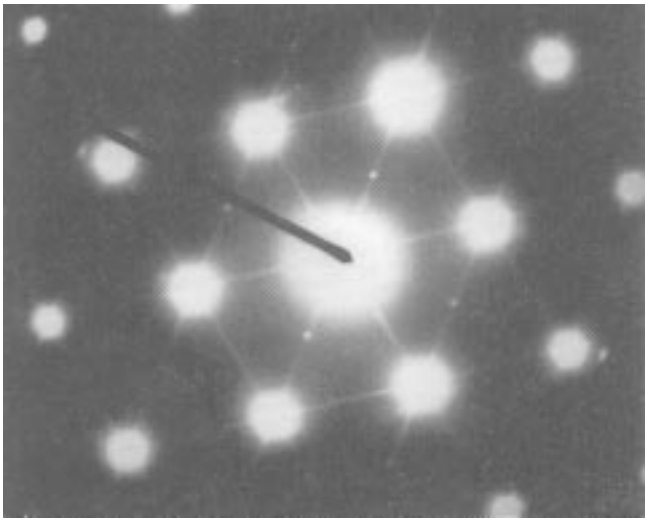

(b)

Fig. 8 Transmission electron microscopy selected area diffraction pattern of matrix microstructure of (a) treatment No. 3 (conventional aging) and (b) treatment No. 4 (multistep heating-rate controlled, or MSRC, aging) . Camera length 150 cm

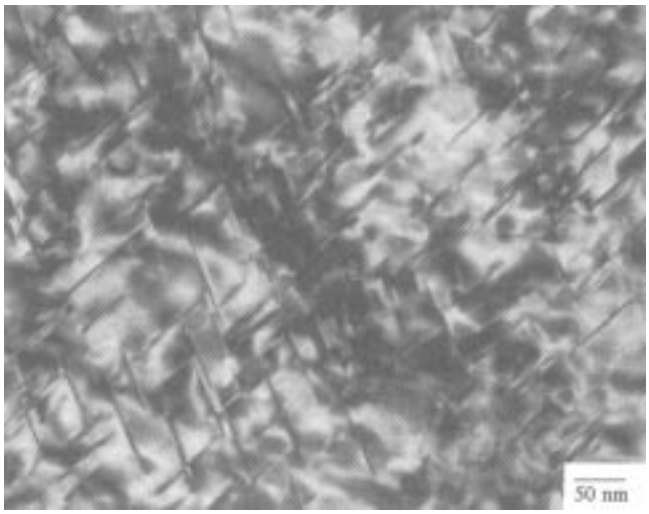

(a)

(b)

Fig. 9 Transmission electron microscopy micrographs showing matrix microstructure of (a) treatment No. 3 (conventional aging) and (b) treatment No. 4 (multistep heating-rate controlled, or MSRC, aging). Note numerous θ′′ with plate diameters <10 nm in (b) as a result of MSRC aging.

electron microscopy bright field micrographs confirmed this observation, showing more θ″ produced by MSRC aging than by conventional aging (Fig. 9). The intensity of diffraction spots for other phases (such as T_1, δ′, θ″) were comparable for both aging techniques. However, MSRC aging appears to promote finer T_1 precipitates. Therefore, MSRC aging is believed to enhance the nucleation of T_1 precipitate, as it did for θ″.

A substantial difference was found in the subgrain boundary microstructures. In the conventionally aged alloy, T_1 had a higher density in the subgrain boundaries than in the matrix (Fig. 10). In the MSRC aged alloy, the grain boundaries were mostly devoid of T_1, and the subgrain boundaries were generally separated by pile-up dislocations (Fig. 10b). Where T_1 occasionally existed at subgrain boundaries, it was not as dense as T_1 precipitate in the matrix. This significant finding clearly showed that MSRC aging can produce the same hardness levels as conventional aging while preventing substantial T_1 precipitation at subgrain boundaries.

4.2 Mechanical Properties and Fractography

Various heat treatments were tested for tensile and fracture toughness (Table 2) (Fig. 11). Increases in YS progressively reduced fracture toughness at ambient temperature for all specimens (Fig. 11). This trend is consistent with behavior observed in most aluminum-lithium alloys, in which toughness generally decreases as strength increases. However, this decrease was not as marked in the MSRC aged alloy as in the conventionally aged alloy. When YS exceeded 510 MPa (74 ksi), cryogenic toughness decreased drastically as strength increased. Cryogenic toughness at high strength levels was considerably improved by the MSRC aging treatment, which can be optimized to increase fracture toughness by more than 15%.

In order to further evaluate the repeatability and effectiveness of this new aging treatment, testing was performed on three more lots of Alloy 2195 (lots B, C, D) that received aging treatments No. 3 and 4. Again, the new aging treatment demonstrated its effectiveness in improving CFT and FTR and significantly improved the cryogenic fracture toughness values (Fig. 12).

Fracture surfaces of the conventionally aged alloy were primarily transgranular at ambient temperature (Fig. 13). However, intergranular fracture increased when YS exceeded 517 MPa (75 ksi) and significantly increased at –196 °C (–320 °F). MSRC aged alloy displayed fracture surfaces that were primarily transgranular, regardless of strength level or test environment. (Compare Fig. 13a and 12b, which show overload fracture regions immediately adjacent to the precrack boundaries.)

Table 2 Aging treatment and mechanical properties of Alloy 2195 (lot A)

Treatment No.	Yield strength, MPa	Ultimate tensile strength, MPa	Elongation, %	Ambient K_{IC}(MPa $\sqrt{m}$)	Cryogenic K_{IC}(MPa $\sqrt{m}$)	Fracture toughness ratio (cryogenic/ambient)(a)
1	520.0	544.1	7.4	34.25	31.83	0.93
2	531.0	530.3	8.1	30.59	30.35	0.99
3	520.1	538.6	7.9	33.78	33.18	0.98
4	531.2	533.1	7.9	33.41	34.84	1.04
5	509.6	531.7	10.5	34.07	37.26	1.09

(a) Ratio of cryogenic toughness to ambient temperature toughness

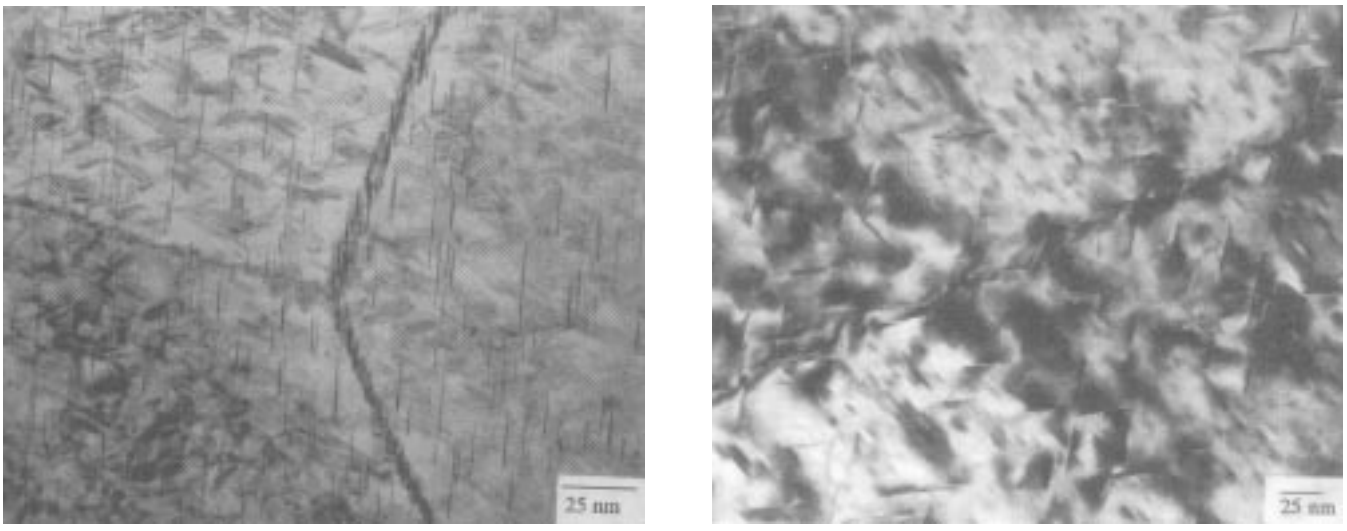

(a) **(b)**

Fig. 10 Transmission electron microscopy micrographs showing subgrain boundary microstructure of (a) treatment No. 3 (conventional aging) and (b) treatment No. 4 (multistep heating-rate controlled, or MSRC, aging). Note much higher density of T_1 precipitate in (a) due to conventional aging.

5. Discussion

This study demonstrates that appropriate aging treatment can be used to control the microstructure of aluminum-lithium alloys, resulting in higher fracture toughness at cryogenic than ambient temperature. Fracture toughness is known to be directly related to microstructure and YS at ambient temperature. However, little information is available to correlate cryogenic toughness and FTR to microstructure. The literature on aluminum alloys suggests that temperature can improve, deteriorate, or fail to affect their fracture toughness, depending on chemical composition, microstructure, and stress state (Ref 7, 8). In this study, the chemical composition and stress states were identical, and the only variable was microstructure.

Here, the conventionally aged alloy developed a significantly decreased FTR and fracture toughness at a YS of 531 MPa (77 ksi) (Fig. 10). The MSRC aged alloy retained a positive FTR (~1.04) at nearly the same YS. This difference can be explained by differences found in the microstructures of these alloys, as all specimens had the same chemical compositions

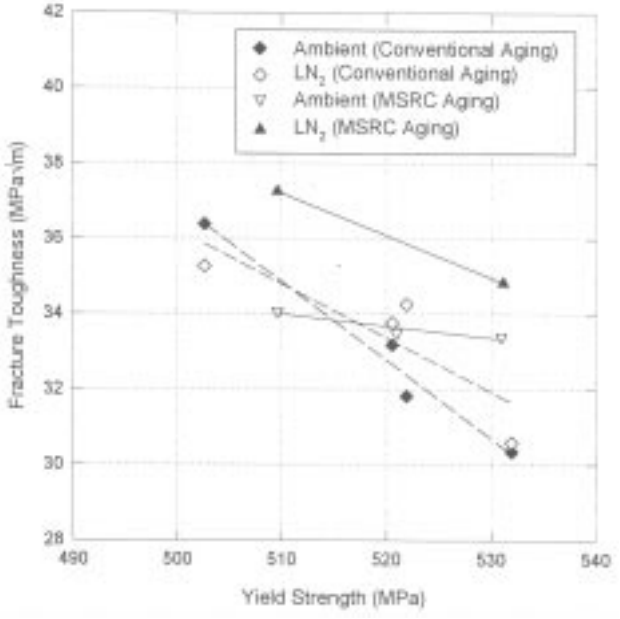

Fig. 11 Fracture toughness improves at the same level of yield strength at ambient and cryogenic temperatures

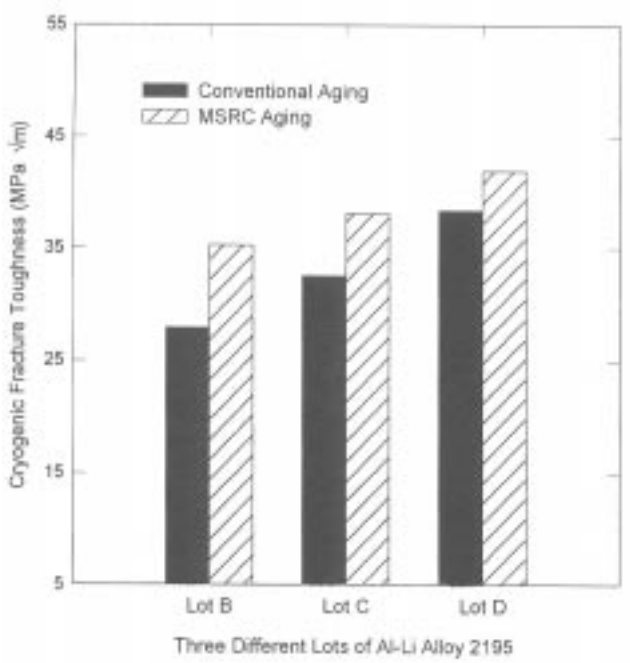

Fig. 12 Cryogenic fracture toughness data for lot B, C, and D, obtained using conventional (treatment No. 3) and multistep heating-rate controlled (MSRC) aging (treatment No. 4). As shown, the MSRC aging can improve cryogenic fracture toughness by up to 26%, depending on the original toughness values.

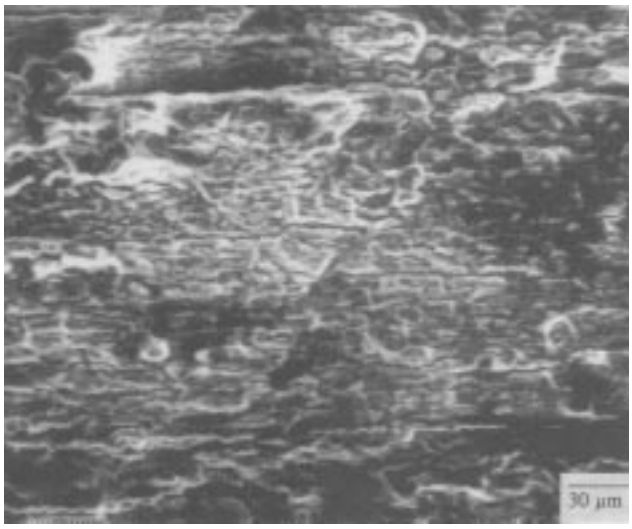

(a)

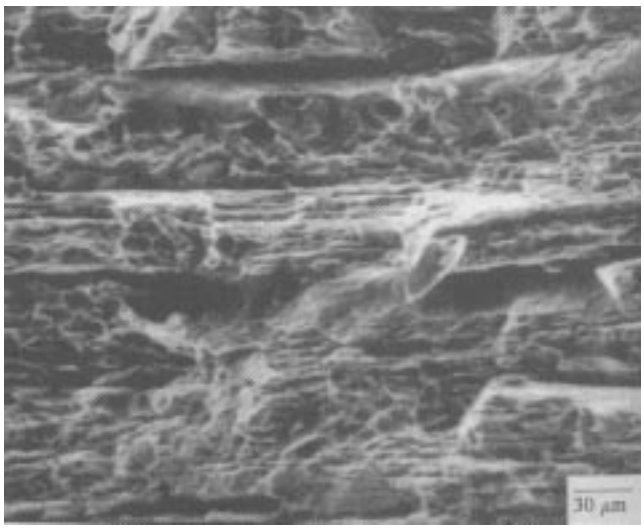

(b)

Fig. 13 Scanning electron microscopy images of microscopic appearance, showing distribution of intergranular and transgranular area in (a) conventional aged specimen (treatment No. 3) and (b) multistep heating-rate controlled aged specimen (treatment No. 4)

and stress states. Their major difference lies in subgrain boundary precipitation, because MSRC aging changes the size and distribution of strengthening precipitates in the grain interior and subgrain boundaries. Conventional and MSRC aging produce different mechanical properties that can be qualitatively correlated to microstructural characteristics (e.g., type, size, distribution, and density of strengthening phases T_1 and θ″). The total number of embryos that can precipitate increases as temperature decreases. Thus, initial holding at low temperature (with high undercooling) is expected to increase the number of precipitate embryos. The low heating rate 0.556 °C/h (1 °F/h) permits sufficient time for embryos to grow above a certain critical size, whereupon they become stable nuclei that continue to grow during the course of aging without considerable dissolution into solid solution. If only two-step isothermal aging is used, the embryos that form at lower temperatures are subject to dissolution at higher temperatures, due to the difference in solid solubility.

During MSRC aging, continuous heating enables precipitate particles to coarsen slowly without dissolving, thereby decreasing the total number of precipitates. As temperatures continue to rise, T_1 will eventually nucleate at subgrain boundaries and start to grow. However, this treatment allows matrix T_1 to precipitate and grow before the subgrain boundary T_1 precipitates do. Early coarsening of matrix T_1 greatly reduces the concentration of matrix copper and lithium, hindering the growth of subgrain boundary T_1 in a diluted Al-Cu-Li solid solution.

Multistep heating-rate controlled aging improves fracture toughness at ambient temperature, which can be explained by a series of observations that fit with a simple model based on the damaging effect of grain boundary precipitates, as developed by Embury and Nes (Ref 9). Their model predicts the value of fracture toughness in materials containing a high area fraction of incoherent grain boundary precipitates in a soft precipitate-free zone (PFZ) of unspecified width. They suggest that, when the grain boundary shear strain γ_f reaches a critical value (given by $\gamma_f \approx [(1/A_f)^{0.5} - 1]/2$ where A_f is the area fraction of incoherent grain boundary precipitates), the voids around each particle coalesce, whereupon the sample fractures. The energy absorbed upon fracture G_C ($\sim K_C^2/E$, with E being the elastic modulus) should be given by $G_C = \sigma^*\gamma_f \approx \sigma^* [(1/A_f)^{0.5} - 1]/2$ (Ref 9), where σ* was taken as a stress in the order of the ultimate tensile strength (UTS). Unwin and Smith (Ref 10) also observed that K_C^2 increased linearly with $(1/A_f)^{0.5}$. A similar trend was observed in this study, where MSRC aging led to improvements in fracture toughness that were much more significant at cryogenic than at ambient temperature.

In aluminum-lithium alloys, improved cryogenic toughness has been correlated to such factors as solidification of low-melting point impurities (Ref 11), reduced strain localization in closer and more widely spaced slip bands (Ref 12), increased homogeneity of plastic deformation from increased strain hardening capacity (Ref 13), and delaminating toughening on fracture surfaces (Ref 14, 15). However, these mechanisms do not account for observed differences in the relationship between grain boundary precipitation and toughness in alloys with different aging treatments. Because alloy chemistry, thermomechanical processing, grain size, and YS remained unchanged, the only factors that could affect the toughness were matrix and grain boundary precipitates.

Fractographic examination showed that better fracture toughness accompanied a change from intergranular to transgranular fracture, which suggests that subgrain boundary precipitates are responsible. In aluminum alloys, temperature may improve, deteriorate, or fail to affect the strength-toughness relationship. In Alloy 2195, fracture toughness generally increases as temperature decreases, due to YS and ultimate tensile strength (UTS) increases, strain hardening exponent, and fracture strain. These trends could reverse when substantial amounts of precipitates occur at the grain boundaries.

This study strongly suggests that Alloy 2195 has inherently positive FTR, with fracture toughness that should always be higher at cryogenic than at ambient temperature if T_1 precipitation can be prevented at subgrain boundaries. It is not clear whether clean subgrain boundaries alone can account for this toughness, but subgrain boundary precipitates are present in low-toughness material and absent in high-toughness material.

Thus, subgrain boundary precipitation is probably the most important factor influencing cryogenic fracture toughness. The presence of subgrain boundary precipitates may be due to alloy composition, as well as microstructural changes produced by TMP (i.e., degree of recrystallization and grain size) or heat treatment (i.e., solutioning and aging treatments). Alloy properties could be considerably impacted by any change in subgrain boundary microstructure produced by these factors. Therefore, as a precautionary measure, subgrain boundary precipitation should be avoided in alloys intended for cryogenic service conditions.

6. Summary

- Size and density of T_1 precipitates at subgrain boundaries are major contributors to fracture toughness and FTR. A MSRC aging treatment for solution-treated and stretched Alloy 2195 improves fracture toughness at cryogenic temperatures. The MSRC aging allows T_1 to nucleate preferentially in the matrix and grow steadily without returning to solution, reduces growth kinetics of subgrain boundary T_1 (as well as the timespan available for its growth), and decreases T_1 distribution density at subgrain boundaries.
- This MSRC aging treatment achieves high strength by promoting T_1 and θ′ nucleation in the matrix so the total number density of precipitates is higher than that seen in conventionally aged materials.
- The MSRC aging treatment reduces the length of time that the materials are exposed to high temperatures, constraining T_1 nucleation and growth at subgrain boundaries and permitting the material to achieve much improved cryogenic fracture toughness.

References

1. J.R. Pickens, W.T. Tack, F.W. Gayle, and J.R. Maisano, *Proceedings of the 1994 Conference on Advanced Earth-to-Orbit Propulsion Technology,* NASA/MSFC, 57, 1994
2. P.S. Chen, "TEM Investigation on Fracture Toughness Variation in Al-Li Alloy 2195," IITRI/MRF, NASA/MSFC, 1994

3. C.P. Blankenship, Jr. and E.A. Starke, Jr., *Acta Metall.*, Vol 42, 1995, p 845
4. J.R. Pickens, "Atlas of Microstructures for Weldalite," Martin Marietta Laboratories, 1991
5. D.A. Porter and K.E. Easterling, *Phase Transformation in Metals and Alloys*, 2nd ed., Chapman & Hall, 1992, p 276
6. R.E. Reed-Hill, *Physical Metallurgy Principles*, Brooks/Cole Engineering Division, 1973, p 368
7. K.T. Venkateswara Rao, W. Yu, and R.O. Ritchie, *Metall. Trans. A*, Vol 20, 1989, p 485
8. K.T. Venkateswara Rao, W. Yu, and R.O. Ritchie, *Symposium on Alloy Phase and Stability and Design, Conf. Proc.*, San Francisco, CA, Materials Research Society, G.M. Stocks, D.P. Pope, and A.F. Giamei, Ed., 18-20 April, 1990
9. J.D. Embury and E. Nes, *Z. Metall.*, Vol 65, 1974, p 45
10. P.T. Unwin and G.C. Smith, *J. Inst. Met.*, Vol 97, 1969, p 299
11. D. Webster, *Metall. Trans. A*, Vol 18, 1987, p 2181
12. K.V. Jata and E.A. Starke, Jr., *Scr. Metall.*, Vol 22, 1988, p 1553
13. J. Glazer, S.L. Verzasconi, R.R. Sawtell, and J.W. Morris, Jr., *Metall. Trans. A*, Vol 18, 1987, p 1695
14. Y.B. Xu, L. Wang, Y. Zhang, Z.Z. Wang, and Q.Z. Hu, *Metall. Trans. A*, Vol 22, 1991, p 723
15. K.T.V. Rao, W. Yu, and R.O. Ritchie, *Metall. Trans. A, Vol 20*, 1989, p 485